This is the accepted manuscript made available via CHORUS. The article has been published as:

Quasiparticle relaxation dynamics in URu_{2−x}Fe_{x}Si_{2} single crystals

Peter Kissin, Sheng Ran, Dylan Lovinger, Verner K. Thorsmølle, Noravee Kanchanavatee, Kevin Huang, M. Brian Maple, and Richard D. Averitt

Phys. Rev. B **99**, 165144 — Published 29 April 2019

DOI: 10.1103/PhysRevB.99.165144

Quasiparticle Relaxation Dynamics in $URu_{2-x}Fe_xSi_2$ Single Crystals

Peter Kissin,[1] Sheng Ran,[1,2,*] Dylan Lovinger,[1] Verner K. Thorsmølle,[1] Noravee Kanchanavatee,[1,2,†] Kevin Huang,[2,3,‡] M. Brian Maple,[1,2] and Richard D. Averitt[1,§]

[1] *Department of Physics, University of California San Diego, 9500 Gilman Drive, La Jolla, California 92093, USA*
[2] *Center for Advanced Nanoscience, University of California San Diego, La Jolla, California 92093, USA*
[3] *Materials Science and Engineering Program, University of California San Diego, 9500 Gilman Drive, La Jolla, California 92093, USA*

(Dated: March 20, 2019)

We investigate quasiparticle relaxation dynamics in $URu_{2-x}Fe_xSi_2$ single crystals using ultrafast optical-pump optical-probe (OPOP) spectroscopy as a function of temperature and Fe substitution (x), crossing from the hidden order (HO) phase ($x = 0$) to the large moment antiferromagnet (LMAFM) phase ($x = 0.12$). At low temperature, the dynamics for $x = 0$ and $x = 0.12$ are consistent with the low energy electronic structure of the HO and LMAFM phases that emerge from the high temperature paramagnetic (PM) phase. In contrast, near the bicritical point separating HO and LMAFM ($x = 0.1$), two transitions occur over a narrow temperature range (from 15.5 - 17.5 K). A PM to HO transition occurs at an intermediate temperature followed by a transition to the LMAFM phase at lower temperature. While the data at low temperatures are consistent with the expected coexistence of LMAFM and HO, the data in the intermediate temperature phase are not, and instead suggest the possibility of an unexpected coexistence of HO and PM. Additionally, the dynamics in the PM phase reflect the presence of a hybridization gap as well as strongly interacting spin and charge degrees of freedom. OPOP yields insights into meV-scale electrodynamics with sub-Kelvin temperature resolution, providing a complementary approach to study low energy electronic structure in quantum materials.

I. INTRODUCTION

The metallic actinide compound URu_2Si_2, with its many proximal phases, offers a platform to study emergent phenomena in f-electron systems poised between localization and itinerancy. In particular, the hidden order (HO) phase, which develops from a strongly correlated paramagnetic (PM) phase below $T_0 = 17.5$ K[1,2], has attracted extensive attention[3]. The combined efforts of ARPES[4–7], quantum oscillations[8], and band structure calculations[9,10] have led to a consistent picture of the Fermi surface. Neutron scattering measurements have identified magnetic excitations at $Q_0 = (1, 0, 0)$ and $Q_1 = (1 \pm 0.4, 0, 0)$ in the body-centered tetragonal Brillouin zone (BZ) of the PM phase, which are gapped in the HO phase[11,12]. Despite this progress, the order parameter of the HO phase remains unidentified, motivating novel experimental approaches.

An alternate route to understanding HO is to instead study the large-moment antiferromagnetic (LMAFM) phase in pressurized URu_2Si_2[13]. While the LMAFM and HO phases have similar signatures in thermodynamics and transport[14], and nearly identical Fermi surfaces[8], the order parameter and symmetries of the LMAFM phase are known, facilitating progress in theory[10]. Unfortunately, even the modest pressure necessary to access LMAFM renders many techniques impossible. However, substitution of Fe for Ru yields an antiferromagnetic phase without applied pressure[15,16]. Striking resemblances exist between the magnetic excitation spectra of the two phases[17], and distinctive features of the phase diagrams of URu_2Si_2 are reproduced[18,19]. Apparently, Fe substitution acts as a chemical pressure, enabling new measurements in the LMAFM phase[20].

Optical Pump Optical Probe (OPOP) spectroscopy has been used to study quasiparticle (QP) relaxation dynamics in a diverse array of systems, including heavy fermion compounds with hybridization gaps[21,22], as well as in Kondo insulators[23,24], heavy fermion superconductors[25], cuprates[26–28], Fe-based superconductors[29], BCS superconductors[30], charge and spin density wave compounds[31,32], and even recently in strongly spin-orbit coupled systems such as iridates[33] and ruthenates[34]. The versatility of this technique comes from its extreme sensitivity to the formation of meV-scale gaps in the electronic density of states (DOS) near the Fermi Energy E_F. The population of QPs that are excited across-gap by the pump pulse results in a small change in the occupied joint density of states, altering the optical properties of the sample as measured by the time-delayed probe pulse[35]. The meV-scale QP relaxation dynamics can then be studied using optical or near-IR probe beams if at least one selection rule allowed interband transition involving a gapped band is available at the probe photon energy. The presence of a gap can then be inferred from the temperature (T) and pump fluence (F) dependence of the QP relaxation dynamics and may result in an increase in the relaxation time by several orders of magnitude at low temperature.

In this study, we investigate QP relaxation dynamics in $URu_{2-x}Fe_xSi_2$ single crystals spanning a broad range of Fe substitution (x), focusing on the compositions indicated in Fig. 1. We observe differences in the dynamics between the HO ($x = 0$) and LMAFM ($x = 0.12$)

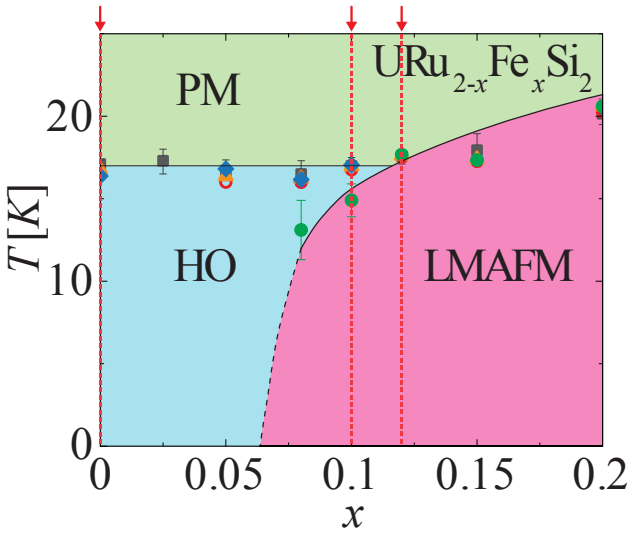

Figure 1: Phase diagram of $URu_{2-x}Fe_xSi_2$, reproduced from[18]. Transition temperatures determined by resistivity, magnetization, and heat capacity are depicted by gray squares, red rings, and orange triangles, respectively. Thermal expansion shows two transitions, which are depicted by blue diamonds and green circles. Optical pump-probe data are presented on samples with $x = 0$, $x = 0.1$, and $x = 0.12$, indicated by the red dashed lines and arrows.

phases, which are successfully described using a simple phenomenological model of relaxation bottlenecks associated with gaps characteristic of each state. In contrast, near the bicritical point separating HO and LMAFM (x = 0.1), two transitions occur over a narrow temperature range (from 15.5 - 17.5 K). A PM to HO transition occurs at higher temperature, with a subsequent transition to a LMAFM phase at lower temperature. While signatures of heterogeneity are present in both phases, anomalies in the intermediate temperature HO phase suggest the unusual possibility of a persistent PM volume fraction. In the PM phase, the dynamics reveal the presence of a hybridization gap as well as strongly interacting spin and charge degrees of freedom.

II. EXPERIMENTAL TECHNIQUES

A schematic of the experiment is shown in Fig. 2. Our laser system consists of an amplified Yb fiber laser, producing 350 fs pulses centered at 1040 nm. 4 W of 1040 nm is frequency doubled to 520 nm and used to pump a non-collinear optical parametric amplifier with two amplification stages. This yields several hundred mW of power depending on signal wavelength, tunable from 650-900 nm, with a bandwidth-limited pulse duration of less than 20 fs. We use an acousto-optic modulator made of quartz to modulate the pump beam for lock-in detection of the signal. Quartz has reduced chromatic dispersion compared to the more common TeO_2, allowing for recompression of the pump pulse with a simple prism pair. The acousto-optic modulator is synchronized with a subharmonic of the laser repetition rate, so that every pump pulse is either diffracted or blocked. Achromatic focusing on to the sample is accomplished using an off-axis parabolic mirror. The cross polarized pump and probe beams were focused to $\frac{1}{e^2}$ spot diameters of 100 μm and 60 μm respectively.

Balanced photodiodes are used to enhance the dynamic range of detection and to partially remove shot-to-shot fluctuations of the laser intensity from the signal. We find that balanced detection increases the smallest signal we can resolve by slightly less than an order of magnitude. Small long term drifts in the balance, which reduce the effectiveness of cancellation, arise from temperature dependent changes in reflectivity, changes in the position of beam on sample, formation of ice on the sample surface, etc. In order to correct for this drift, the 209 kHz pulsetrain from each photodiode is integrated, producing a DC signal. The two DC signals are subtracted, producing a difference signal that drives a servo motor. The servo motor adjusts the position of an ND filter placed in the reference beam path in order to set the intensity of the reference beam equal to that of the signal beam. The DC signal from the sample photodiode is sent to the auxiliary channel of lock-in amplifier for continuous measurement of the reflectivity R.

The Fe-substituted single crystals were grown in a tetra-arc furnace using the Czochralski technique[18]. OPOP measurements used 20 fs laser pulses centered at 800 nm with a repetition rate of 209 kHz. The data were collected from large, flat areas of samples cleaved in the a-b plane and immediately placed in vacuum of 10^{-6} mbar or lower inside a continuous flow liquid He optical cryostat. Additional data collected on polished samples showed qualitatively different dynamics at low temperatures, highlighting the importance of studying HO on strain-free regions.

The use of an intermediate repetition rate amplifier has several advantages over the more common 80 MHz oscillator for low temperature OPOP measurements. For an 80 MHz system, cumulative heating due to the average optical power incident upon the illuminated spot is a large source of uncertainty in temperature even at low fluence. In contrast, the repetition rate of 209 kHz is more than two orders of magnitude lower, allowing us to study a wider range of fluences without cumulatively heating the sample at low temperature. This effect likely accounts for the qualitative difference in fluence and temperature dependence between our data and the previous OPOP data on the parent compound reported by Liu *et al.*[36].

The pump fluence was fixed at 0.5 μJ/cm^2 for all temperature dependent measurements to ensure minimal heating of the sample. At this fluence, analysis of the specific heat reported in[2] bounds the change in quasiequilibrium temperature in the sample to less than 4 K at T = 5 K and by less than 0.5 K just below $T_0 \approx$16.5 K in the

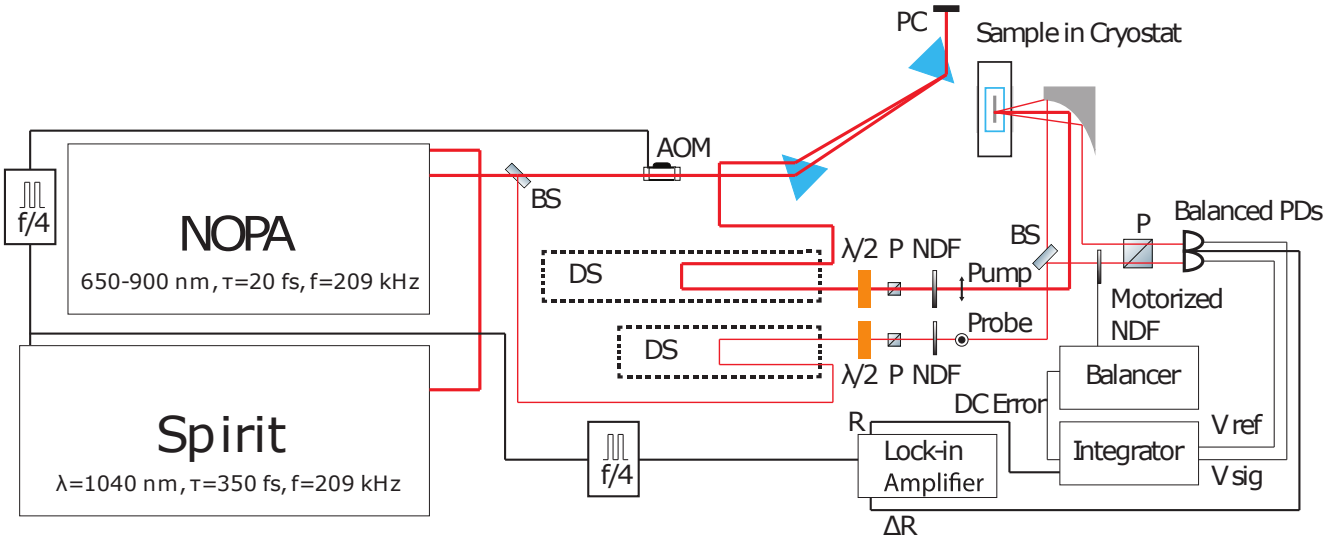

Figure 2: Schematic of experiment. BS = beamsplitter, AOM = acousto-optic modulator, PC = prism compressor, DS = delay stage, $\lambda/2$ = half waveplate. P = polarizer, NDF = continuously variable neutral density filter. PD = photodiode.

parent compound. The number of quasiequilibrium e-h pairs created is an alternate way to assess the strength of photoexcitation. Assuming the 7 meV gap feature in optical conductivity at 5 K[37–41] roughly corresponds to the energy of the QP excitation to which our OPOP measurements are sensitive, we estimate that 0.002 e-h pairs/U atom are excited by the pump pulse at this fluence. This is an order of magnitude lower than the thermal carrier density inside the HO phase of 0.02 e-h pairs/U atom[42], ensuring that our temperature dependent measurements are performed in the weak photoexcitation regime.

III. RESULTS AND DISCUSSION

A. Overview of the Dynamics

Fig. 3 shows the photoinduced change in fractional reflectivity ΔR/R as a function of time. The dynamics are qualitatively similar for all samples. At high temperature, the relaxation is biexponential, consisting of a fast, negative component with a time constant of hundreds of fs and a small, slow, positive component with a time constant of hundreds of ps. Upon cooling, the fast component begins to slow to the few ps timescale, and the slower component switches sign and increases in amplitude. At T_0, between 17 K and 16.5 K, the signal amplitude continues to increase for a few ps after photoexcitation and the relaxation time approaches a ns. These abrupt changes to the dynamics at T_0 mark the transition to the low temperature phase.

We fit the data with a multiexponential function:

$$\frac{\Delta R}{R}(t) = f(t) * (A_f e^{-t/\tau_f} + A_s e^{-t/\tau_s} + C) \quad (1)$$

Where $f(t) = 0.5 * (1 - erf[-\sigma(t - t_0)]) * (1 + A_r(1 - e^{-(t-t_0)/\tau_r}))$. In $f(t)$, the first term containing the error function represents the fast rise present at all temperatures. This term is included for completeness and σ is temperature independent. The term containing A_r and τ_r represents the slow rise dynamics that onset below T_0. The second term in Eqn. 1 contains two exponential decays and a constant. The constant is close to the experimental noise floor of 10^{-6} at all temperatures, so our analysis will focus on the temperature dependence of the parameters from the exponential terms. In order to compare amplitudes above and below T_0, we define $(1 + A_r)A_{f,s} = A_{1,2}$ ($\tau_{f,s} = \tau_{1,2}$ for consistency).

B. Fluence Dependence

Fig. 4 shows the fluence dependence of the data covering more than an order of magnitude, roughly centered on $F = 0.5$ μJ/cm^2, above and below T_0, for x = 0.1. The data is normalized to highlight the overlap of all the of the curves, showing that the relaxation dynamics are independent of fluence. At higher fluence, above roughly $F = 2$ μJ/cm^2, some fluence dependence is observed both above and below T_0. Below T_0, this can be understood as the fluence necessary to quench the HO phase. Following the quench of the HO phase, the relaxation dynamics will be qualitatively different than the relaxation dynamics of photoexcited QPs within the HO

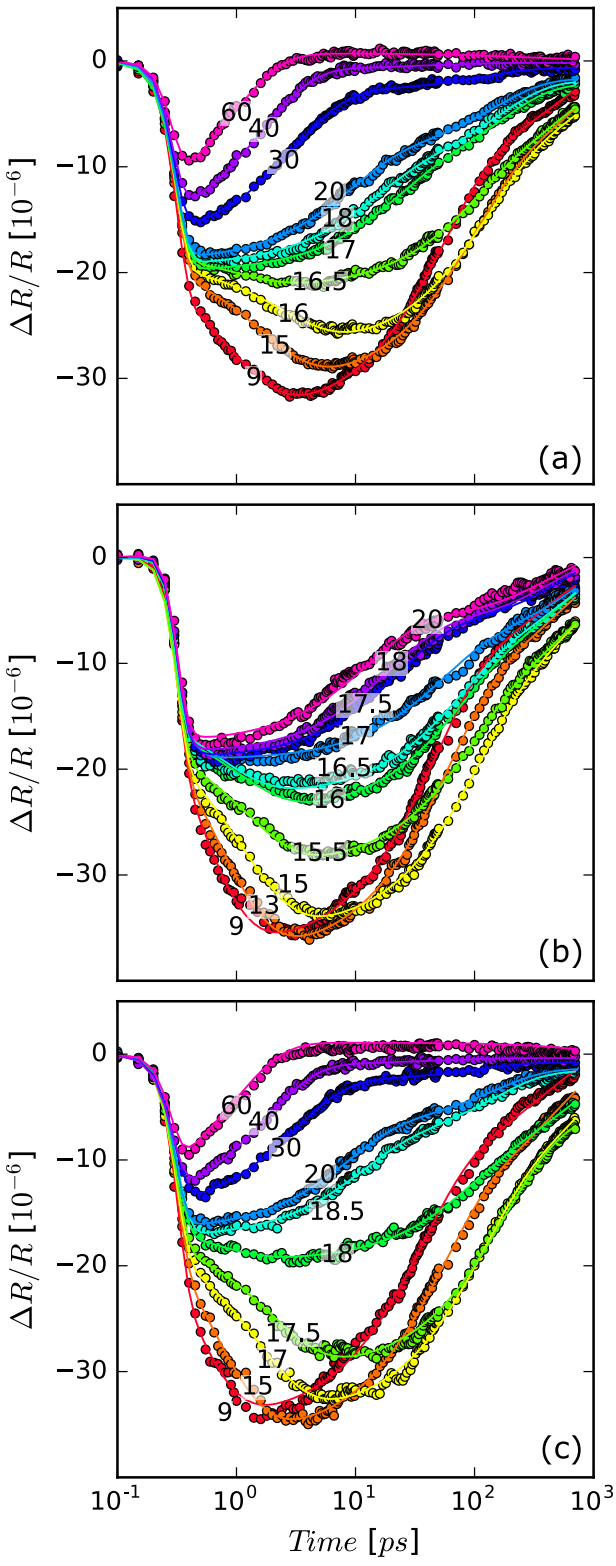

Figure 3: Fractional change in reflectivity ΔR/R vs. time after photoexcitation for $x = 0$. Each curve is labelled by the corresponding temperature in Kelvin. Solid lines are fits to the data using Eqn. 1. (a) $x = 0$, (b) $x = 0.1$, (c) $x = 0.12$

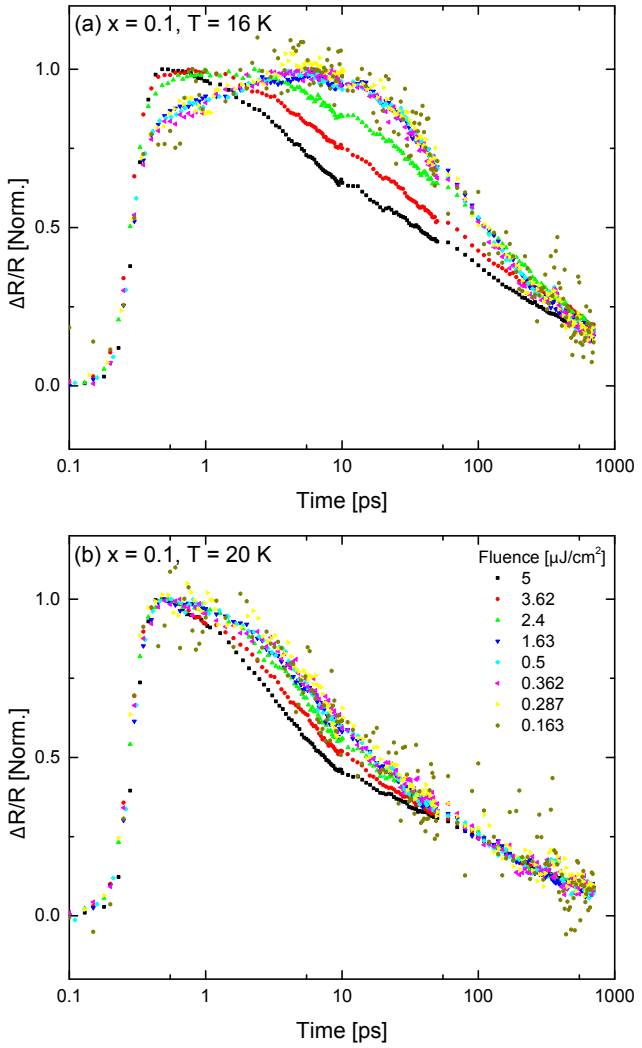

Figure 4: Fluence dependence of the QP relaxation dynamics (a) at $T = 16$ K, and (b) at $T = 20$ K.

phase. The origin of the fluence dependence in the PM phase will be discussed later.

Relaxation of photoexcited QPs in the presence of a gap requires e-h recombination with the emission of a high energy boson (HEB) with energy $\hbar\omega \geq E_{gap}$. This situation is frequently analyzed using the phenomenological Rothwarf-Taylor (RT) model[43]. The key parameters in the RT model are the bare QP recombination rate γ_r, the rate of across-gap QP excitation by a HEB γ_{pc}, and the rate of escape or anharmonic decay of HEBs γ_{esc}. Various regimes are realized depending on these rates[29,44]. If $\gamma_r \gg \gamma_{pc}$ or $\gamma_{esc} \gg \gamma_{pc}$, then bimolecular recombination dynamics are observed, and the bare recombination rate of QPs γ_r can be obtained. On the other hand, if γ_{pc} is the fastest rate, the result is a strong bottleneck with a relaxation rate limited to γ_{esc}. The observation of fluence independent relaxation dynamics below roughly $F = 2$ μJ/cm^2 in Fig. 4 implies strongly

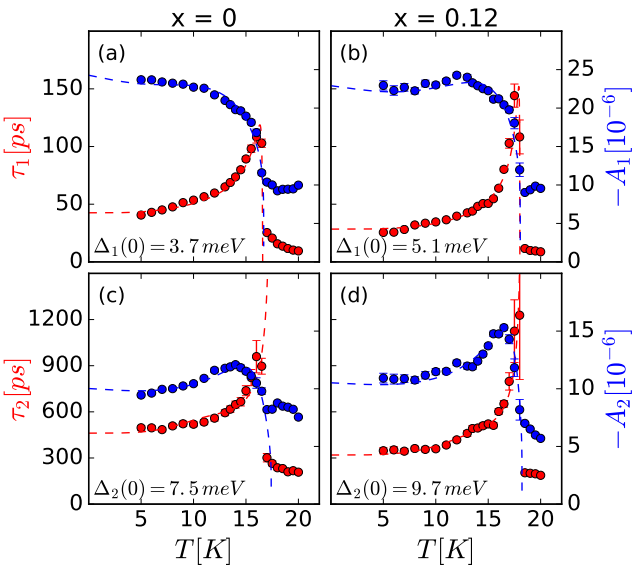

Figure 5: Temperature dependence of fit parameters below T_0. A_1 and τ_1 vs. T for (a) $x = 0$ and (b) $x = 0.12$. A_2 and τ_2 vs. T for (c) $x = 0$ and (d) $x = 0.12$. Blue and red dashed lines are fits to Eqn. 2 and Eqn. 3, respectively. Gap energies extracted by these fits are displayed.

bottlenecked QP relaxation.

C. Dynamics in the Hidden Order and Large Moment Antiferromagnetic Phases

Fig. 5 shows the parameters extracted from fits to the raw data using Eqn. 1 below 20 K. All time constants diverge approaching T_0 from below and jump to lower values in the PM phase. This divergence is characteristic of a bottleneck associated with a temperature dependent gap where the limiting step is the anharmonic decay of HEBs[26,45]. To analyze the temperature dependence of the fit parameters, we use a bottleneck model due to Kabanov *et al.*[35]:

$$A(T) = \frac{F/(\Delta(T) + k_B T/2)}{1 + \gamma\sqrt{\frac{2k_B T}{\pi\Delta(T)}}exp[-\Delta(T)/k_B T]} \qquad (2)$$

$$\frac{1}{\tau(T)} = \frac{K\Delta(T)^2}{ln(1/\{c\Delta(0)^2 + exp[-\Delta(T)/k_B T]\})} \qquad (3)$$

In Eqn. 2 and Eqn. 3, $F \propto \mathcal{E}_I$, $\gamma = 2\nu/N(0)\hbar\Omega_c$, $K = 12\Gamma_\omega/\hbar\omega^2$, $c = \mathcal{E}_I/2N(0)$. $\mathcal{E}_I$ is the photoexcited energy density per unit cell, ν is the number of modes per unit cell, and $N(0)$ is the electronic DOS at E_F. Ω_c, Γ_ω, and ω are the cutoff frequency, linewidth, and frequency of the modes, respectively. Eqn. 2 and Eqn. 3 can be derived from the RT model in the strong bottleneck regime. The temperature dependence of the gaps is modeled with a generic BCS form $\Delta(T) = \Delta(0)tanh(1.74\sqrt{(T/T_0 - 1)})$[39,40]. We treat the zero-temperature gap $\Delta(0)$ and the transition temperature T_0 as shared parameters and fit to Eqn. 2 and Eqn. 3 simultaneously, strongly constraining the extracted values of $\Delta(0)$.

Fits to the fast component, shown in (a) and (b) of Fig. 5, yield smaller gap energies than reported with optical techniques, $\Delta_1(0) = 3.7 \pm 0.1$ meV for $x = 0$ and $\Delta_1(0) = 5.1 \pm 0.2$ meV for $x = 0.12$. An indirect gap is a possibility, since infrared and Raman spectroscopy only probe direct gaps. The energies roughly agree with the energies of the magnetic excitation at Q_1, which has been interpreted as an interband transition across an indirect hybridization gap[12,17]. A hybridization gap bottleneck arises naturally from this interpretation.

Fits to the slow component, shown in (c) and (d), return values of $\Delta_2(0) = 7.5 \pm 0.5$ meV and $\Delta_2(0) = 9.7 \pm 1.1$ meV for $x = 0$ and $x = 0.12$, respectively. These values are consistent with measurements of the charge gaps in the HO and LMAFM phases of Fe-substituted samples[15,16,46]. The value for $x = 0$ also agrees with the HO gap from Raman spectroscopy[47,48], so we interpret the slow component as a bottleneck involving a direct gap between a localized, occupied f-state and a light conduction band that crosses the E_F as in[48].

The gap energies extracted by the fits shown in Fig. 5 correspond to the literature values for both phases. This excellent agreement supports the description of the QP relaxation dynamics in terms of bottlenecks using Eqn. 2 and Eqn. 3 and demonstrates the sensitivity of our technique to the low energy electronic structure of URu_2Si_2. Clearly, we can distinguish between the QP relaxation dynamics in the HO and LMAFM phases, even though the gaps of the two phases differ by only a few meV.

D. Anomalous Temperature Dependence Near the Bicritical Point

Armed with an understanding of the dynamics for $x = 0$ and $x = 0.12$, we turn to the fit parameters for $x = 0.1$, shown in Fig. 6. Anomalous temperature dependence is observed between 17.5 K and 15.5 K. Both time constants jump twice: once between 17.5 and 17 K at T_0, and again at a second temperature T_1 between 16 and 15.5 K. In contrast, abrupt changes in relaxation times occur only once, at T_0, for both $x = 0$ and $x = 0.12$. Additionally, the rise in amplitudes below T_0 occurs more gradually for $x = 0.1$ than for $x = 0$ or $x = 0.12$, with a discontinuity in slope at T_1. These observations are reminiscent of thermal expansion measurements[18], where the two phase transitions observed for $x = 0.08$ and $x = 0.1$ were interpreted as a second order PM to HO transition and a first order HO to LMAFM transition.

One particularly striking feature of the data is the abrupt increase in signal amplitude observed at the HO and LMAFM transitions. We perform a model-independent comparison of the low temperature behav-

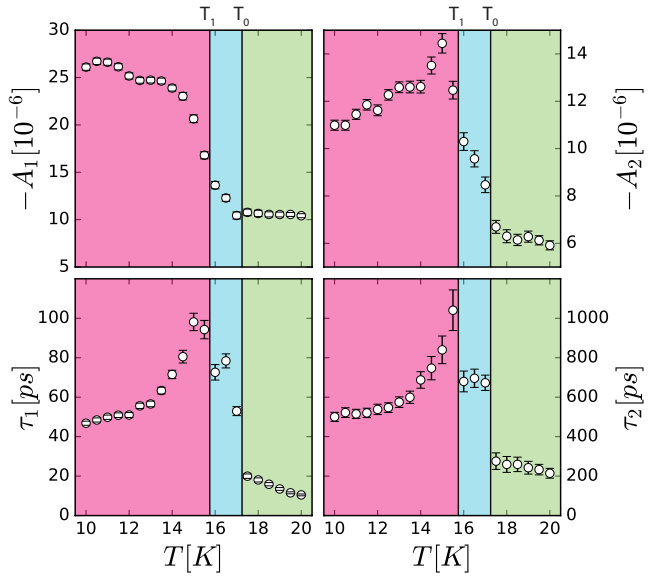

Figure 6: temperature dependence of fit parameters below T_0 for $x = 0.1$. The data from the proposed LMAFM, HO, and PM phases are highlighted in red, blue, and green, respectively.

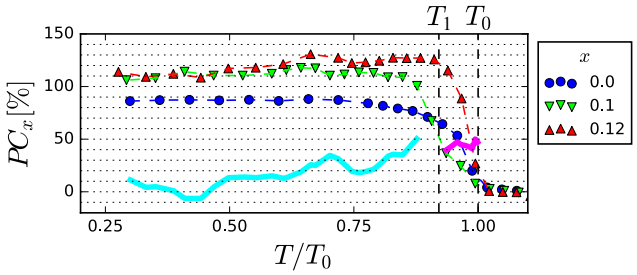

Figure 7: Percent change in OPOP signal amplitude PC_x vs. reduced temperature T/T_0 for $x = 0$, $x = 0.1$, and $x = 0.12$. Dashed colored lines are interpolations between adjacent data points. Dashed vertical lines are estimates for T_0 and T_1. The solid cyan line is an estimated HO volume fraction V_{HO} below T_1. The solid magenta line is an estimated PM volume fraction V_{PM} between T_0 and T_1 based on the possible phase coexistence between HO and PM. V_{HO} and V_{PM} are listed as percentages to facilitate plotting on the same axes.

ior of all three samples by considering the percentage change in the signal amplitude, $PC_x(T)$, *with respect to the PM phase*, in which the dynamics are independent of x. Specifically, we consider the quantity $PC_x(T) = (A_x(T) - (A_x(20K))/(A_x(20K)$, where $A_x(T)$ denotes the raw signal amplitude for sample x at temperature T. Since the PM component of the signal is independent x and varies relatively slowly with temperature, $PC_x(T)$ has the approximate form of a percentage change of the signal amplitude due to the emergence of HO or LMAFM order for each sample. These quantities are plotted for each sample as a function of reduced temperature T/T_0 in Fig. 7. For $x = 0$, the amplitude nearly doubles as the sample cools from the PM phase to the HO phase (corresponding to a percentage change of nearly 100%). The increase is even greater for LMAFM phase in $x = 0.12$.

The well documented coexistence of HO and LMAFM domains in the parent compound[49,50] originates from inhomogeneous strain due to defects[51], and is thus likely to be enhanced around Fe sites, as in the case of Rh substituted samples[52]. This effect likely plays a much larger role for $x = 0.1$, given its proximity to the HO/LMAFM phase boundary, than for either $x = 0$ and $x = 0.12$. Therefore, in order to study inhomogeneity in $x = 0.1$, we assume that $x = 0$ and $x = 0.12$ represent comparatively pure HO and LMAFM phases, respectively.

Below T_1, the data for $x = 0.1$ matches expectations. Since the amplitude in Eq. 2 depends only on band structure and lattice parameters[35], the overlap between $PC_{0.1}(T)$ and $PC_{0.12}(T)$ suggests that $x = 0.1$ and $x = 0.12$ have the same phase composition at low temperature. Closer to T_1, $PC_0(T) < PC_{0.1}(T) < PC_{0.12}(T)$. This is expected behavior for coexisting HO and LMAFM domains, with a HO volume fraction V_{HO} that decreases with temperature. So, we assume that the signal for $x = 0.1$ in this temperature range consists of HO regions with volume fraction V_{HO} and LMAFM regions with volume fraction $1 - V_{HO}$, which may be expressed as $V_{HO} = (PC_{0.12} - PC_{0.1})/(PC_{0.12} - PC_0)$. As seen in Fig. 7, V_{HO} decreases roughly linearly, from $V_{HO} \approx 0.5$ just below T_1 to $V_{HO} \approx 0$ at low temperature. In contrast, it is difficult to describe the data for $x = 0.1$ between T_0 and T_1 in terms of coexistence between HO and LMAFM. Here, the expected phase composition is primarily HO with a small LMAFM volume fraction. However, $PC_{0.1}(T)$ is less than expected for both pure HO and LMAFM.

We speculate that the anomalously small signal amplitude arises from phase coexistence of PM and HO. For example, if we assume that the signal for $x = 0.1$ contains contributions from HO and PM domains, we may write $V_{PM} = (PC_0 - PC_{0.1})/PC_0$. From this, we obtain an estimate for a PM volume fraction $V_{PM} \approx 0.5$, which is strikingly close to V_{HO} just below T_1. There are several reasonable explanations for this unusual possibility. Perhaps the PM to HO transition in this sample is driven weakly first order by proximity to the bicritical point in the phase diagram or by disorder from Fe substitution. On the other hand, there is evidence for a weakly first order PM to HO transition in the parent compound[53], and a first order PM to HO transition was predicted in a recent theoretical study[54]. It is also possible that this is a nonequilibrium effect, similar to the coexistence between superconducting and normal state domains observed in photoexcited superconductors[55–57]. Each of these outcomes points to exotic and novel physics in f-electron systems, meriting future studies to replicate this observation and to clarify its origin, if confirmed.

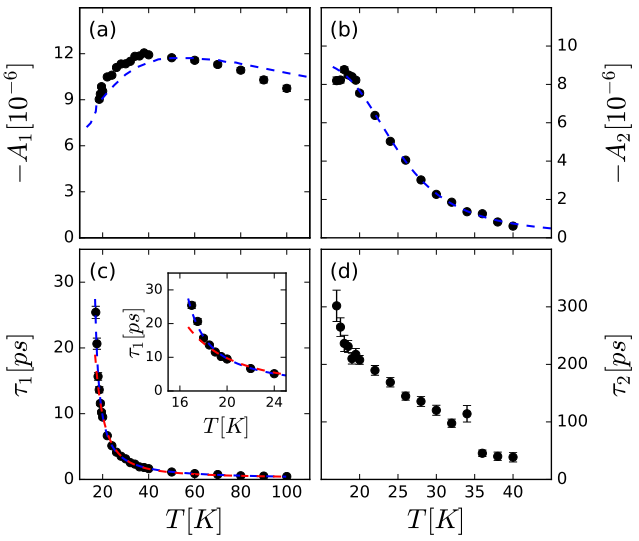

Figure 8: temperature dependence of fit parameters in the PM phase for $x = 0$. (a) A_1 vs. T. The blue dashed line is the c-axis magnetic susceptibility from[2], scaled for comparison. (b) A_2 vs. T. The blue dashed line is a fit to Eq. 2 with a temperature independent gap[35]. (c) τ_1 vs. T. The blue and red dashed lines are fits to a power law and a bottleneck model, respectively, as described in the text. The inset shows the same quantities plotted over a narrower temperature range, from 15 K to 25 K. (d) τ_2 vs. T.

E. Dynamics in the Paramagnetic Phase

The data in the PM phase is also informative. We first discuss the temperature dependence of A_2, shown in Fig. 8(b). In a previous OPOP study on the parent compound[36], this component was interpreted as evidence of a HO pseudogap[58–60]. The dynamics we observe are nearly independent of x in the PM phase. This observation is likely incompatible with a HO pseudogap that arises from competition between HO and LMAFM phases, but does not rule out scenarios where the HO pseudogap originates from fluctuations of a shared HO-LMAFM order parameter above T_0[20,61]. On the other hand, a fit of A_2 to a temperature independent form of Eq. 2 between T_0 and 40 K, shown in Fig. 8(b), is consistent with a bottleneck associated with a gap of 13.8±0.5 meV. This is likely the correct interpretation of this component, since a hybridization gap of similar energy has been observed in the PM phase with a number of techniques[39,40,58,62].

Next, we discuss the fast process A_1 and τ_1. As shown in Fig. 5, A_1 peaks near 40 K and decreases upon approaching T_0. This is not the expected behavior from a bottleneck. At this fluence, we assume that the concentration of photoexcited QPs is much less than the concentration of thermal QPs $n_S \ll n_T$ and approximate $\tau^{-1}(T) = C[n_S + n_T] \approx Cn_T$, with $n_T = T^{1/2}e^{-\Delta/kT}$. A fit to this equation, shown in red in Fig. 5(c), returns a gap value of Δ=4.9±0.1 meV. This value does not match any charge gap reported in the literature above T_0.

On the other hand, the resemblance between A_1 and the c-axis magnetic susceptibility, highlighted in Fig. 5(a), indicates that the fast process may have a magnetic origin. A power law fit[63] of the form $\tau_1(T) \propto ((T - T_0)/T_0)^{-k}$, shown in Fig. 5(c), reproduces the temperature dependence of τ_1, particularly the quasi-divergence near T_0, with $k = 1.14 \pm 0.05$ and $T_0 = 14.5 \pm 0.4$ K. The slight disagreement between the nominal and extracted values of T_0 is likely due to pump induced heating that limits the accuracy of transition temperatures and critical exponents measured with this technique. It is this same effect that is responsible for the fluence dependence shown in Fig. 4(b), where the initial relaxation process is faster at higher fluence. Nonetheless, the value for the scaling exponent k is close to the exponent describing critical slowing down in the 3D Ising model, $\nu z = 1.28 \pm 0.03$[64,65], where ν is the critical exponent of correlation length and z is the dynamical critical exponent[66]. The 3D Ising model is a good starting point to describe magnetic fluctuations in the PM phase given the notable Ising anisotropy in URu_2Si_2[67].

Based on this analysis, we conclude that the fast process tracks a relaxation channel for photoexcited QPs involving scattering with magnetic fluctuations that slows as the magnetic fluctuations become critical. The literature supports this interpretation. Strong magnetic fluctuations are present at both Q_0[68] and Q_1[11] in this temperature range, and nearly critical behavior of magnetic fluctuations at Q_0 has been reported[61]. The THz frequency scattering of carriers by critical magnetic fluctuations can also explain the non-Fermi liquid behavior observed in the PM state[69].

IV. CONCLUSION

To conclude, our measurements of QP relaxation dynamics in the $URu_{2-x}Fe_xSi_2$ single crystals reveal several new insights. The dynamics in the PM phase, which are nearly independent of x, highlight the presence of a hybridization gap as well as the influence of strong interactions between QPs and critical magnetic fluctuations. Below T_0, the dynamics in the HO and LMAFM phases reflect known differences in the low energy electronic structure. As in past measurements[18], we observe a second phase transition in a sample of intermediate Fe substituent concentration $x = 0.1$. In addition to a low temperature LMAFM phase, there is a distinct intermediate temperature HO phase. The anomalous data in this phase suggests the unexpected possibility of coexisting HO and PM. Our study lays the groundwork for future experiments on the $URu_{2-x}Fe_xSi_2$ system to understand HO, its relationship to LMAFM, and novel forms of order in f-electron systems more generally.

ACKNOWLEDGMENTS

This research was supported by the U.S. National Science Foundation under Grant No. DMR-1810310 (ultrafast optical pump-probe spectroscopy measurements and materials characterization), the U.S. Department of Energy, Office of Science, Office of Basic Energy Sciences under Award Number DE-FG02-04ER46105 (crystal growth), and ARO W911NF-16-1-0361 (ultrafast instrumentation development).

---

* Present Addresses: Center for Nanophysics and Advanced Materials, Department of Physics, University of Maryland, College Park, MD 20742; NIST Center for Neutron Research, National Institute of Standards and Technology, 100 Bureau Drive, Gaithersburg, MD 20899.

† Present Address: Department of Physics, Chulalongkorn University, Pathumwan, 10330, Thailand.

‡ Present Address: National High Magnetic Field Laboratory, Florida State University, Tallahassee, FL 32313.

§ Corresponding Author:raveritt@ucsd.edu

[1] T. T. M. Palstra, A. A. Menovsky, J. v. d. Berg, A. J. Dirkmaat, P. H. Kes, G. J. Nieuwenhuys, and J. A. Mydosh, Phys. Rev. Lett. **55**, 2727 (1985).

[2] M. B. Maple, J. W. Chen, Y. Dalichaouch, T. Kohara, C. Rossel, M. S. Torikachvili, M. W. McElfresh, and J. D. Thompson, Phys. Rev. Lett. **56**, 185 (1986).

[3] J. A. Mydosh and P. M. Oppeneer, Rev. Mod. Phys. **83**, 1301 (2011).

[4] J.-Q. Meng, P. M. Oppeneer, J. A. Mydosh, P. S. Riseborough, K. Gofryk, J. J. Joyce, E. D. Bauer, Y. Li, and T. Durakiewicz, Phys. Rev. Lett. **111**, 127002 (2013).

[5] C. Bareille, F. L. Boariu, H. Schwab, P. Lejay, F. Reinert, and A. F. Santander-Syro, Nature Communications **5**, 4326 (2014).

[6] S. Chatterjee, J. Trinckauf, T. Hänke, D. E. Shai, J. W. Harter, T. J. Williams, G. M. Luke, K. M. Shen, and J. Geck, Phys. Rev. Lett. **110**, 186401 (2013).

[7] F. L. Boariu, C. Bareille, H. Schwab, A. Nuber, P. Lejay, T. Durakiewicz, F. Reinert, and A. F. Santander-Syro, Phys. Rev. Lett. **110**, 156404 (2013).

[8] E. Hassinger, G. Knebel, T. D. Matsuda, D. Aoki, V. Taufour, and J. Flouquet, Phys. Rev. Lett. **105**, 216409 (2010).

[9] S. Elgazzar, J. Rusz, M. Amft, P. M. Oppeneer, and J. Mydosh, Nature Materials **8**, 337 (2009).

[10] P. M. Oppeneer, J. Rusz, S. Elgazzar, M.-T. Suzuki, T. Durakiewicz, and J. A. Mydosh, Phys. Rev. B **82**, 205103 (2010).

[11] C. R. Wiebe, J. A. Janik, G. J. MacDougall, G. M. Luke, J. D. Garrett, H. D. Zhou, Y.-J. Jo, L. Balicas, Y. Qiu, J. R. D. Copley, Z. Yamani, and W. J. L. Buyers, Nature Physics **3**, 96 (2007).

[12] N. P. Butch, M. E. Manley, J. R. Jeffries, M. Janoschek, K. Huang, M. B. Maple, A. H. Said, B. M. Leu, and J. W. Lynn, Phys. Rev. B **91**, 035128 (2015).

[13] G. Motoyama, T. Nishioka, and N. K. Sato, Phys. Rev. Lett. **90**, 166402 (2003).

[14] E. Hassinger, G. Knebel, K. Izawa, P. Lejay, B. Salce, and J. Flouquet, Phys. Rev. B **77**, 115117 (2008).

[15] N. Kanchanavatee, M. Janoschek, R. E. Baumbach, J. J. Hamlin, D. A. Zocco, K. Huang, and M. B. Maple, Phys. Rev. B **84**, 245122 (2011).

[16] P. Das, N. Kanchanavatee, J. S. Helton, K. Huang, R. E. Baumbach, E. D. Bauer, B. D. White, V. W. Burnett, M. B. Maple, J. W. Lynn, and M. Janoschek, Phys. Rev. B **91**, 085122 (2015).

[17] N. P. Butch, S. Ran, I. Jeon, N. Kanchanavatee, K. Huang, A. Breindel, M. B. Maple, R. L. Stillwell, Y. Zhao, L. Harriger, and J. W. Lynn, Phys. Rev. B **94**, 201102 (2016).

[18] S. Ran, C. T. Wolowiec, I. Jeon, N. Pouse, N. Kanchanavatee, B. D. White, K. Huang, D. Martien, T. DaPron, D. Snow, M. Williamsen, S. Spagna, P. S. Riseborough, and M. B. Maple, Proceedings of the National Academy of Sciences **113**, 13348 (2016).

[19] S. Ran, I. Jeon, N. Pouse, A. J. Breindel, N. Kanchanavatee, K. Huang, A. Gallagher, K.-W. Chen, D. Graf, R. E. Baumbach, J. Singleton, and M. B. Maple, Proceedings of the National Academy of Sciences **114**, 9826 (2017).

[20] H.-H. Kung, S. Ran, N. Kanchanavatee, V. Krapivin, A. Lee, J. A. Mydosh, K. Haule, M. B. Maple, and G. Blumberg, Phys. Rev. Lett. **117**, 227601 (2016).

[21] J. Demsar, R. D. Averitt, K. H. Ahn, M. J. Graf, S. A. Trugman, V. V. Kabanov, J. L. Sarrao, and A. J. Taylor, Phys. Rev. Lett. **91**, 027401 (2003).

[22] K. S. Burch, E. E. M. Chia, D. Talbayev, B. C. Sales, D. Mandrus, A. J. Taylor, and R. D. Averitt, Phys. Rev. Lett. **100**, 026409 (2008).

[23] J. Demsar, V. K. Thorsmølle, J. L. Sarrao, and A. J. Taylor, Phys. Rev. Lett. **96**, 037401 (2006).

[24] J. Demsar, J. L. Sarrao, and A. J. Taylor, Journal of Physics: Condensed Matter **18**, R281 (2006).

[25] D. Talbayev, K. S. Burch, E. E. M. Chia, S. A. Trugman, J.-X. Zhu, E. D. Bauer, J. A. Kennison, J. N. Mitchell, J. D. Thompson, J. L. Sarrao, and A. J. Taylor, Phys. Rev. Lett. **104**, 227002 (2010).

[26] J. Demsar, R. Hudej, J. Karpinski, V. V. Kabanov, and D. Mihailovic, Phys. Rev. B **63**, 054519 (2001).

[27] N. Gedik, P. Blake, R. C. Spitzer, J. Orenstein, R. Liang, D. A. Bonn, and W. N. Hardy, Phys. Rev. B **70**, 014504 (2004).

[28] J. P. Hinton, J. D. Koralek, G. Yu, E. M. Motoyama, Y. M. Lu, A. Vishwanath, M. Greven, and J. Orenstein, Phys. Rev. Lett. **110**, 217002 (2013).

[29] D. H. Torchinsky, G. F. Chen, J. L. Luo, N. L. Wang, and N. Gedik, Phys. Rev. Lett. **105**, 027005 (2010).

[30] J. Demsar, R. D. Averitt, A. J. Taylor, V. V. Kabanov, W. N. Kang, H. J. Kim, E. M. Choi, and S. I. Lee, Phys. Rev. Lett. **91**, 267002 (2003).

[31] J. Demsar, K. Biljaković, and D. Mihailovic, Phys. Rev. Lett. **83**, 800 (1999).

[32] E. E. M. Chia, J.-X. Zhu, H. J. Lee, N. Hur, N. O. Moreno, E. D. Bauer, T. Durakiewicz, R. D. Averitt, J. L. Sarrao, and A. J. Taylor, Phys. Rev. B **74**, 140409 (2006).

[33] H. Chu, L. Zhao, A. de la Torre, T. Hogan, S. D. Wilson, and D. Hsieh, Nature Materials **16**, 200 EP (2017).

[34] Y. Yuan, P. Kissin, D. Puggioni, K. Cremin, S. Lei, Y. Wang, Z. Mao, J. M. Rondinelli, R. D. Averitt, and V. Gopalan, arXiv e-prints , arXiv:1901.02512 (2019),

arXiv:1901.02512 [cond-mat.str-el].
[35] V. V. Kabanov, J. Demsar, B. Podobnik, and D. Mihailovic, Phys. Rev. B **59**, 1497 (1999).
[36] M. K. Liu, R. D. Averitt, T. Durakiewicz, P. H. Tobash, E. D. Bauer, S. A. Trugman, A. J. Taylor, and D. A. Yarotski, Phys. Rev. B **84**, 161101 (2011).
[37] D. A. Bonn, J. D. Garrett, and T. Timusk, Phys. Rev. Lett. **61**, 1305 (1988).
[38] W. T. Guo, Z. G. Chen, T. J. Williams, J. D. Garrett, G. M. Luke, and N. L. Wang, Phys. Rev. B **85**, 195105 (2012).
[39] N. Bachar, D. Stricker, S. Muleady, K. Wang, J. A. Mydosh, Y. K. Huang, and D. van der Marel, Phys. Rev. B **94**, 235101 (2016).
[40] R. P. S. M. Lobo, J. Buhot, M. A. Méasson, D. Aoki, G. Lapertot, P. Lejay, and C. C. Homes, Phys. Rev. B **92**, 045129 (2015).
[41] J. S. Hall, U. Nagel, T. Uleksin, T. Rõ om, T. Williams, G. Luke, and T. Timusk, Phys. Rev. B **86**, 035132 (2012).
[42] Y. Kasahara, T. Iwasawa, H. Shishido, T. Shibauchi, K. Behnia, Y. Haga, T. D. Matsuda, Y. Onuki, M. Sigrist, and Y. Matsuda, Phys. Rev. Lett. **99**, 116402 (2007).
[43] A. Rothwarf and B. N. Taylor, Phys. Rev. Lett. **19**, 27 (1967).
[44] V. V. Kabanov, J. Demsar, and D. Mihailovic, Phys. Rev. Lett. **95**, 147002 (2005).
[45] R. P. S. M. Lobo, J. D. LaVeigne, D. H. Reitze, D. B. Tanner, Z. H. Barber, E. Jacques, P. Bosland, M. J. Burns, and G. L. Carr, Phys. Rev. B **72**, 024510 (2005).
[46] J. S. Hall, M. R. Movassagh, M. N. Wilson, G. M. Luke, N. Kanchanavatee, K. Huang, M. Janoschek, M. B. Maple, and T. Timusk, Phys. Rev. B **92**, 195111 (2015).
[47] J. Buhot, M.-A. Méasson, Y. Gallais, M. Cazayous, A. Sacuto, G. Lapertot, and D. Aoki, Phys. Rev. Lett. **113**, 266405 (2014).
[48] H.-H. Kung, R. E. Baumbach, E. D. Bauer, V. K. Thorsmølle, W.-L. Zhang, K. Haule, J. A. Mydosh, and G. Blumberg, Science **347**, 1339 (2015).
[49] K. Matsuda, Y. Kohori, T. Kohara, K. Kuwahara, and H. Amitsuka, Phys. Rev. Lett. **87**, 087203 (2001).
[50] H. Amitsuka, K. Tenya, M. Yokoyama, A. Schenck, D. Andreica, F. Gygax, A. Amato, Y. Miyako, Y. K. Huang, and J. Mydosh, Physica B: Condensed Matter **326**, 418 (2003).
[51] M. Yokoyama, H. Amitsuka, K. Tenya, K. Watanabe, S. Kawarazaki, H. Yoshizawa, and J. A. Mydosh, Phys. Rev. B **72**, 214419 (2005).
[52] S.-H. Baek, M. J. Graf, A. V. Balatsky, E. D. Bauer, J. C. Cooley, J. L. Smith, and N. J. Curro, Phys. Rev. B **81**, 132404 (2010).
[53] S. Tonegawa, S. Kasahara, T. Fukuda, K. Sugimoto, N. Yasuda, Y. Tsuruhara, D. Watanabe, Y. Mizukami, Y. Haga, T. D. Matsuda, E. Yamamoto, Y. Onuki, H. Ikeda, Y. Matsuda, and T. Shibauchi, Nature Communications **5**, 4188 (2014).
[54] P. Shen and M. Dzero, Phys. Rev. B **98**, 125131 (2018).
[55] C. Giannetti, G. Coslovich, F. Cilento, G. Ferrini, H. Eisaki, N. Kaneko, M. Greven, and F. Parmigiani, Phys. Rev. B **79**, 224502 (2009).
[56] G. Coslovich, C. Giannetti, F. Cilento, S. Dal Conte, G. Ferrini, P. Galinetto, M. Greven, H. Eisaki, M. Raichle, R. Liang, A. Damascelli, and F. Parmigiani, Phys. Rev. B **83**, 064519 (2011).
[57] R. Matsunaga and R. Shimano, Phys. Rev. Lett. **109**, 187002 (2012).
[58] J. Levallois, F. Lévy-Bertrand, M. K. Tran, D. Stricker, J. A. Mydosh, Y.-K. Huang, and D. van der Marel, Phys. Rev. B **84**, 184420 (2011).
[59] J. T. Haraldsen, Y. Dubi, N. J. Curro, and A. V. Balatsky, Phys. Rev. B **84**, 214410 (2011).
[60] K. R. Shirer, J. T. Haraldsen, A. P. Dioguardi, J. Crocker, N. apRoberts Warren, A. C. Shockley, C.-H. Lin, D. M. Nisson, J. C. Cooley, M. Janoschek, K. Huang, N. Kanchanavatee, M. B. Maple, M. J. Graf, A. V. Balatsky, and N. J. Curro, Phys. Rev. B **88**, 094436 (2013).
[61] P. G. Niklowitz, S. R. Dunsiger, C. Pfleiderer, P. Link, A. Schneidewind, E. Faulhaber, M. Vojta, Y.-K. Huang, and J. A. Mydosh, Phys. Rev. B **92**, 115116 (2015).
[62] W. K. Park, P. H. Tobash, F. Ronning, E. D. Bauer, J. L. Sarrao, J. D. Thompson, and L. H. Greene, Phys. Rev. Lett. **108**, 246403 (2012).
[63] Y. Zhu, J. Hoffman, C. E. Rowland, H. Park, D. A. Walko, J. W. Freeland, P. J. Ryan, R. D. Schaller, A. Bhattacharya, and H. Wen, Nature Communications **9**, 1799 (2018).
[64] S. Wansleben and D. P. Landau, Journal of Applied Physics **61**, 3968 (1987).
[65] A. Pelissetto and E. Vicari, Physics Reports **368**, 549 (2002).
[66] P. C. Hohenberg and B. I. Halperin, Rev. Mod. Phys. **49**, 435 (1977).
[67] A. P. Ramirez, P. Coleman, P. Chandra, E. Brück, A. A. Menovsky, Z. Fisk, and E. Bucher, Phys. Rev. Lett. **68**, 2680 (1992).
[68] F. Bourdarot, E. Hassinger, S. Raymond, D. Aoki, V. Taufour, L.-P. Regnault, and J. Flouquet, Journal of the Physical Society of Japan **79**, 064719 (2010).
[69] U. Nagel, T. Uleksin, T. Rm, R. P. S. M. Lobo, P. Lejay, C. C. Homes, J. S. Hall, A. W. Kinross, S. K. Purdy, T. Munsie, T. J. Williams, G. M. Luke, and T. Timusk, Proceedings of the National Academy of Sciences **109**, 19161 (2012).